NUMERICAL SIMULATION OF HIGH REYNOLDS NUMBER FLOWS OVER CIRCULAR CYLINDERS USING THE IMMERSED BOUNDARY METHOD

José Eduardo Santos Oliveira
Laboratory of Heat and Mass Transfer and Fluid Dynamic – University Federal of Uberlândia
Mechanical Engineer College – Bloco 1M – Av. João Naves de Ávila, 2.121. CEP 38400-902
e-mail: jeolivei@mecanica.ufu.br

Ana Lúcia de Lima e Silva
e-mail: alfsilva@mecanica.ufu.br

Francisco José de Souza
e-mail: fjsouza@mecanica.ufu.br

Aristeu da Silveira Neto
e-mail: aristeus@mecanica.ufu.br

Abstract. *In this work an extension of the Immersed Boundary Method with the Virtual Physical Model for simulations of high Reynolds number flows over stationary cylinders is presented. The flow is simulated through the numerical solution of Reynolds Averaged Navier-Stokes Equations and filtered Navier-Stokes equations, using the immersed boundary method to model the cylinder. This methodology, which allows the modeling of immersed complex geometries in the flow, uses two independent meshes: an Eulerian mesh to represent the fluid domain and a Lagrangean mesh for the solid-fluid interface. Two turbulence models have been used: the Smagorinsky subgrid-scale model and the one-equation Spalart-Allmaras turbulent viscosity model. The Smagorinsky model was implemented and used in the context of LES, while the Spalart-Allmaras was implemented and used in the context of URANS and DES. The methodologies LES and DES are, by definition, applied for three-dimensional flows. In the present work they were applied to two-dimensional flows as an approximation. Preliminary results are shown comparing the implemented models results with experimental data.*

Keywords*: Immersed Boundary Method, Cylinders, High Reynolds Flows, Turbulence Modeling*

1. Introduction

Fluid flow over immersed complex geometries always has been one of the main interests in computational fluid dynamics (CFD). In fact, most of the existing real problems involve complex geometries, e.g., bioengineering, aerodynamics, multiphase flow, etc. Two main approaches are being used to handle these problems: the unstructured grid methods and the immersed boundary methods (IB). This last one was proposed by Peskin (1977) to simulate blood flow in heart valves, a high complex problem that involves moving boundaries and complex geometries.

The main idea of the Peskin method is to use two meshes. The Eulerian mesh is used to solve the fluid flow equations while an independent Lagrangean mesh represents the immersed body. The interaction between the two meshes is made through a force source term added to the Navier-Stokes equations. This procedure allows to model complex geometries immersed in a fluid flow, avoiding the use of complex meshes to fit the grid to the immersed body. The main advantages of the immersed boundary method are memory and CPU savings and easy grid generation compared to the unstructured grid method (Kim *et al.* 2001).

The main issue in the methods based on the concept of immersed boundary is how to compute the force term. In the present work, a new model named Virtual Physical Model (VPM) proposed by Lima e Silva *et al.* (2003), is used. It is based on the calculation of the force field over a sequence of Lagrangean points, which represent the interface, using the Navier-Stokes equations. The immersed boundary method, using the Virtual Physical Model, has allowed to obtain good results in simulations of different cases. For example, in problems involving simple geometries, like flows over a stationary circular cylinders, at low Reynolds numbers (Lima e Silva *et al.* 2003); complex flows around bluff bodies and multi-body (Lima e Silva *et al.* 2004). Silva *et al.* (2004) simulated fluid flows over a rotating and oscillating cylinders at Reynolds numbers up to 1000. Arruda (2004) used immersed boundary method to simulate induced flows in an assembly channel-cavity with a periodic moving bottom. Oliveira *et al.* (2004) presented flow simulations around a cylinder of variable diameter in time below critical Reynolds number.

In the present work, the IB/VPM is used to simulate flow over a stationary cylinder at Reynolds numbers above 10^4. Three different turbulence modelling methodologies were used: URANS, DES and LES. To calculate the turbulent viscosity, the Smagorinsky algebraic sub-grid scale model was used to perform LES and the Spalart-Allmaras (S-A) one-equation model to perform URANS and DES. The LES and DES methodologies were used in the two-dimensional approximation. The simulation results were compared between with each other and with the results of others authors.

2. Mathematical Formulation

The main idea in the IB/VPM methodology is to solve the flow over immersed bodies using two independent meshes: a fixed Eulerian mesh for fluid domain and a Lagrangean mesh to represent body-fluid interface. Related to the mesh building, there are no difficulties to represent complex immersed bodies.

2.1. Mathematical Model for Fluid Domain

The fluid domain is always rectangular and is discretized with an Eulerian grid. The flow inside this domain is modeled by the Navier-Stokes equations, Eq. (1), and the continuity equation, Eq. (2), for viscous and incompressible flows:

$$\rho\left[\frac{\partial\left(u_i\right)}{\partial t}+\frac{\partial\left(u_i u_j\right)}{\partial x_j}\right]=-\frac{\partial p}{\partial x_j}+\frac{\partial}{\partial}\left[\left(\nu+\nu_t\right)\left(\frac{\partial u_i}{\partial x_j}+\frac{\partial u_j}{\partial x_i}\right)\right]+f_i, \tag{1}$$

$$\frac{\partial u_i}{\partial x_i}=0. \tag{2}$$

It must be stressed that Eq. (1) is already the filtered Navier-Stokes equation. Also, the Boussinesq hypothesis was used to model the subgrid Reynolds stress tensor. These equations are solved on Eulerian mesh and the coupling between two meshes are made by the force source term f_i that is different from zero only over the immersed boundary. Equation (3) models the interaction between the immersed boundary and the fluid flow, by the distribution of the force field on the fluid:

$$\vec{f}\left(\vec{x}\right)=\int_{\Omega}\vec{F}\left(\vec{x}_k,\ t\right)\delta\left(\vec{x}-\vec{x}_k\right)d\vec{x}_k, \tag{3}$$

where $\vec{F}$ is the Lagrangean force density placed on $\vec{x}_k$ points over the interface and $\delta(\vec{x}-\vec{x}_k)$ is a Dirac delta function.

In order to discretize the Dirac delta function that appears in Eq. (3), it must be replaced by the distribution function D_{ij}. This function acts like a Gaussian weight function with a unitary integral over the interval $[-\infty,+\infty]$. Therefore, Eq. (3) is replaced by:

$$\vec{f}\left(\vec{x}\right)=\sum D_{ij}\left(\vec{x}-\vec{x}_k\right)\vec{F}\left(\vec{x}_k,\ t\right)\Delta s^2, \tag{4}$$

where Δs is the distance between two Lagrangean points.

2.2. Solid-Fluid Interface Model

The VPM performs dynamic evaluation of the force exerted by the fluid flow over the immersed body (see Fig. 1). The force density $\vec{F}(\vec{x}_k,t)$ is calculated over the Lagrangean points using all the Navier-Stokes terms. The Lagrangean force should be expressed by:

$$\vec{F}_i\left(\vec{x}_k,t\right)=\frac{\partial u}{\partial t}+\frac{\partial p}{\partial x_i}+\frac{\partial\left(u_i u_j\right)}{\partial x_j}-\frac{\partial}{\partial x_j}\left[\nu\left(\frac{\partial u_i}{\partial x_j}+\frac{\partial u_j}{\partial x_i}\right)\right]. \tag{5}$$

The different terms on the right side of Eq. (5), are referred to as: acceleration force, pressure force, inertial force and viscous force. The four components of force density $\vec{F}(\vec{x}_k,t)$ are calculated on a control volume centered at a Lagrangean point, as illustrated in Fig. (1).

To evaluate the different terms described by Eq. (5) the pressure $p(\vec{x},t)$ and the velocity $\vec{V}(\vec{x},t)$ fields must be known a priori. These fields are calculated on the Eulerian grid while the force terms must be calculated over the interface. One of the possible ways to do that is to interpolate $\vec{V}(\vec{x},t)$ and $p(\vec{x},t)$ over appropriate auxiliary Lagrangean points near the interface, as illustrated by Lima e Silva *et al.* (2003).

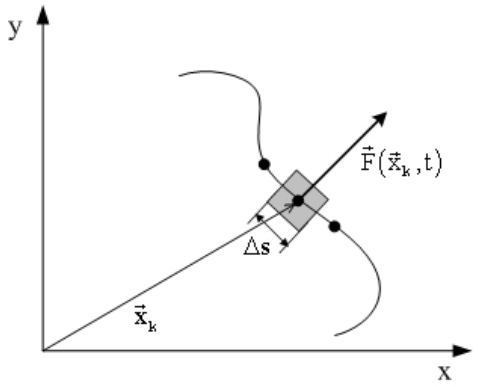

Figure 1. Control volume centered at a generic Lagrangean point.

For pressure field, only external grid points to the interface and at a distance less than or equal to $2\Delta x$ are used in the interpolation process; for the velocity fields external and internal points are taken, because the internal velocity field helps to model virtually the no-slip velocity condition on the immersed boundary. The pressure and velocity derivatives that appear in Eq.(5), are calculated using a second order Lagrange polynomial approximation.

3. Turbulence Modelling

The Navier-Stokes equations are able to simulate, with fairly good agreement, a wild range of engineering problems including high complex unsteady turbulent flows. However, it is necessary to solve all degrees of freedom of the flow, which is proportional to $Re^{9/4}$. This technique is called DNS (*Direct Numerical Simulation*) and it is obviously restricted to low Reynolds number due to the high mesh resolution required, considering the nowadays computers.

An alternative way to handle this problem is the use of Reynolds decomposition or general filtering process of Germano (1986). The governing equations are suitably filtered, this procedure gives rise to the closure problem. This closure problem is nowadays solved using turbulence models. Different methodologies have been employed in the turbulence modeling, based RANS (*Reynolds Averaged Navier-Stokes*) models are considered as the most practical turbulence handling technique with available computational resources (Kapadia and Roy, 2003). The RANS equations are derived by decomposing the dependent variables of Navier-Stokes equations into filtered components and fluctuating components and then filtering all equation terms. It is necessary to use additional assumptions to the closure of equations system, i.e., the turbulence modeling. A common terminology used is the *Unsteady*-RANS (URANS) to refer the classical RANS equations in which the transient terms are added, (Silveira-Neto *et al.,* 2002).

The LES (*Large Eddy Simulation*) methodology is philosophically close to DNS than it is to URANS. The largest turbulent structures are solved from the filtered equations and only the smallest structures are modeled. These small structures are more homogeneous and isotropic (Silveira-Neto, 2003). The scale of the small structure is evaluated from the mesh used to solve the filtered equations, i.e., the filter width becomes a function of the grid. The turbulent structures that are smallest than grid resolution are modeled by the so-called subgrid-scale models.

DES (*Detached Eddy Simulation*) was proposed by Spalart *et al.* (1997). This is a conceptual hybrid method and is not linked to any specific turbulence model. The main idea is combining the best features of URANS and LES and generating a hybrid methodology used as a single model. The URANS model is used in the regions near wall, where these models show good results with less mesh refinement as compared with LES. For regions away from the walls, LES is used, because it is able to predict complex physical phenomena like separated flow.

In the present work two turbulence models, the Smagorinsky subgrid-scale model and a Spalart-Allmaras turbulence model were employed. The formulation of theses models are discussed in the following sections.

3.1. Smagorinsky Sub-grid Scale Model

In the present work LES methodology proposed by Smagorinsky (1963) is applied. The sub-grid scale model, which is based on the balance of production of sub-grid scale turbulent kinetic energy and dissipation of isotropic turbulence energy, is used.

The turbulent viscosity is computed as function of strain rate (S_{ij}) and the length scale (ℓ):

$$\nu_t = (C_s \ell)^2 \sqrt{2\bar{S}_{ij}\bar{S}_{ij}}\,, \tag{6}$$

where $C_S = 0.18$ is the Smagorinsky constant and $\ell = \sqrt{\Delta x \Delta y}$ is the characteristic sub-grid length.

3.2. Spalart-Allmaras Model

Spalart and Allmaras (1994) proposed a new one-equation URANS model (S-A model). This model solves a single transport equation for turbulent viscosity. The equation for the turbulent viscosity is assembled "using empiricism and arguments of dimensional analysis, Galilean invariance and selected dependence on molecular viscosity". This model has being successfully used in aerodynamic flow simulations and separation prediction.

The S-A model uses a work variable $\tilde{\nu}$ given by the following transport equation:

$$\frac{\partial \tilde{\nu}}{\partial t}+\frac{\partial (u_j \tilde{\nu})}{\partial x_j}=c_{b1}\tilde{S}\tilde{\nu}-c_w f_w\left[\frac{\tilde{\nu}}{d_w}\right]^2+\frac{1}{\sigma}\left[\frac{\partial}{\partial x_j}\left((\nu+\tilde{\nu})\frac{\partial \tilde{\nu}}{\partial x_j}\right)+c_{b2}\frac{\partial \tilde{\nu}}{\partial x_j}\frac{\partial \tilde{\nu}}{\partial x_j}\right], \tag{7}$$

where the right side terms represent: turbulence eddy viscosity production, a wall destruction term that reduces the turbulent viscosity in the laminar sublayer, and turbulent and molecular diffusion process. The last term is the turbulent viscosity dissipation. The original S-A model includes also trip terms that provides a smooth transition to turbulence, in the present work trip terms are neglected.

The turbulent viscosity function is defined in terms of a work variable $\tilde{\nu}$ and a wall function f_{v1}, as follows:

$$\nu_t=\tilde{\nu}\cdot f_{v1}\,, \qquad f_{v1}=\frac{\chi^3}{\chi^3+c_{v1}^3} \qquad \textit{and} \qquad \chi\equiv\frac{\tilde{\nu}}{\nu}. \tag{8}$$

The $\tilde{S}$ parameter, from the production term in Eq. (7), can be written as:

$$\tilde{S}\equiv S+\frac{\tilde{\nu}}{(\kappa d_w)^2}f_{v2} \qquad \textit{and} \qquad f_{v2}=1-\frac{\chi}{1+\chi f_{v1}}. \tag{9}$$

where d_w is the distance to the closest wall and S is the magnitude of strain rate. The wall destruction function f_w is:

$$f_w=g\left(\frac{1+c_{w3}^6}{g^6+c_{w3}^6}\right)^{1/6}, \qquad g=r+c_{w2}\left(r^6-r\right) \qquad \textit{and} \qquad r\equiv\frac{\tilde{\nu}}{\tilde{S}\kappa^2 d_w^2}. \tag{10}$$

The model constants are:

$$c_{w1}=\frac{c_{b1}}{\kappa^2}+\frac{(1+c_{b2})}{\sigma}, \qquad c_{w2}=0.3, \qquad c_{w3}=2,$$
$$\kappa=0.41, \qquad c_{v1}=7.1, \qquad \sigma=2/3, \qquad c_{b1}=0.1355, \qquad c_{b2}=0.622. \tag{11}$$

The S-A model was originally based on the URANS philosophy. In this model the distance to the closest wall is used as the length scale d_w. However, in the S-A based DES model the variable d_w is replaced by a new length scale $\tilde{d}$, defined as:

$$\tilde{d}\equiv min\left(d_w,\, C_{DES}\Delta\right) \qquad \textit{where} \qquad \Delta\equiv max\left(\Delta x,\, \Delta y\right). \tag{12}$$

If $\tilde{d}=d_w$, i.e., in boundary layer region, the model works as a standard S-A model. In the regions away from solid boundaries, the length scale becomes grid dependent $\tilde{d}=C_{DES}\Delta$ and the model acts as a subgrid-scale model. When production and destruction terms balance each other, this model reduces to an algebraic Smagorinsky-like model $(\nu\propto\Delta^2 S)$. Shur *et al.* (1999) set the additional model constant $C_{DES}=0.65$ for homogeneous turbulence. This value is used without modification in the present work.

4. Numerical Method

The governing equations, Eq. (1) and (2), were discretized using the central second-order finite difference method in space and a Runge-Kutta second-order scheme in the time. The pressure-velocity coupling was performed using a pressure correction method, as proposed by Chorin (1968).

The linear system for the pressure correction was solved using the iterative solver MSI (*Modified Strongly Implicit Procedure*) of Schneider and Zedan (1981). The interface force field calculation and the momentum equation solution are performed in an explicit way.

All the simulations were carried out on the non-uniform grid. The calculation domain has a length of *50D* and a width of *25D.* These dimensions were chosen in order to minimize the boundary effects on the flow development. A grid refinement study was done to verify the result independence, based on this study the mesh was defined. The non-uniform grid has three distinct regions in each direction, as can be observed with more details in Fig. (2), on the *x* direction the first section has *80* meshes and is extended until *15.5D*, the last section has *32.5D* of length with *140* meshes. In the *y* direction the two non-uniform sections are identical with *11.5D* of length and *96* meshes. Around the cylinder a uniform mesh inside a box of side *2D* is used.

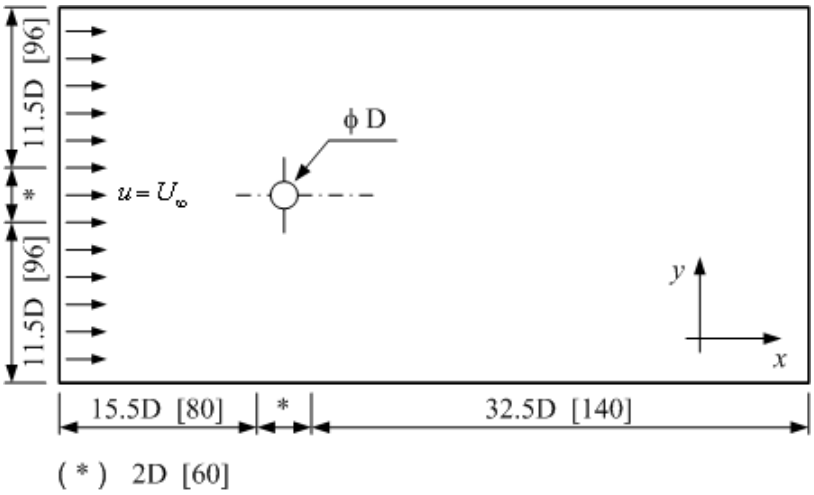

Figure 2. View of the calculation domain.

The immersed cylinder of diameter *D* has its center placed at *16.5D* from the left boundary and centered vertically at *12.5D*, see Fig. (2). A constant velocity profile U_∞ was imposed at the domain inlet, in such a way that the fluid goes from the left to the right boundary. Neumann conditions were imposed for velocity at all other faces. For the pressure correction, null derivative was employed at the domain entrance and it was set as zero in the other faces.

5. Results and Discussions

In this section the preliminary results are presented for the two-dimensional unsteady flow past a circular cylinder. The immersed cylinder was represented by IB/VPM methodology. Three turbulence models (S-A based URANS, S-A based DES and Smagorinsky-LES) where employed to simulate five different Reynolds from 10^4 up to 10^6, two test cases above *drag crisis* region ($Re_D \approx 2\times10^5$) was also simulated.

Figure 3 presents the temporal evolution of the drag and the lift coefficients for a Reynolds number of 10^4. The numerical results are presented for a total non-dimensional time of 180 tU/d with a fixed time step of 0.001, Fig. 3. The mean drag values were calculated only with the last 80 tU/d because the statistical regime is well defined. Figure 3-b shows the lift for the three methodologies. It can be observed that the LES result have higher amplitude of oscillation as compared with URANS and DES but the mean lift coefficient is very close one to the other.

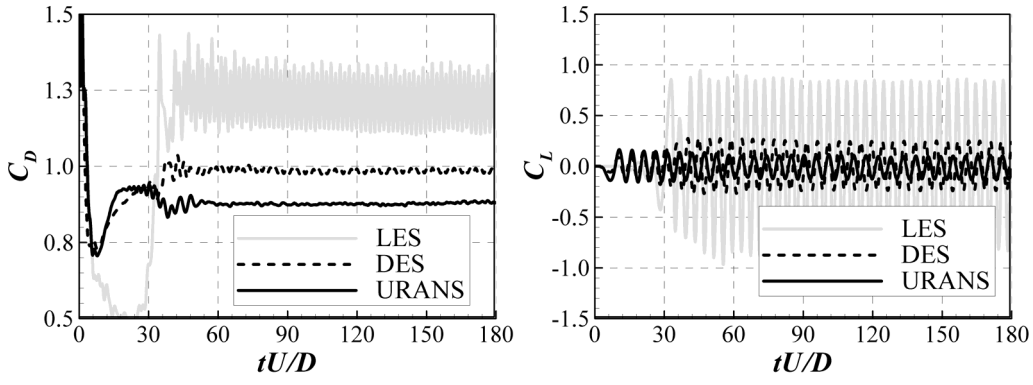

Figure 3. Temporal evolution of the drag (a) and the lift (b) coefficients.

The mean drag coefficient obtained in the present work are shown in Tab. 1 and compared with experimental results from the literature. The Sucker and Brauer correlation (White, 1991) is worth for Reynolds numbers in the range of $1.0\times10^{-4} \le Re_D \le 2.0\times10^{5}$. Above this range the numerical results were compared with the experimental results of Wieselsberger and presented by Schlichting (1979). Figure 4 shows the numerical results compared with the experimental results obtained by Wieselsberger.

Table 1. Drag coefficient obtained with the three methodologies and compared with the experimental ones.

Re_D	Mean Drag Coefficient ($\overline{C}_D$)				
	Present work			Sucker and Brauer (White, 1991)	Wieselsberger (Schlichting, 1979)
	URANS	DES	LES	Curve-fit (Exp. Data)	Exp. Data
1 x 10^4	0.8782	0.9840	1.2203	1.091	1.139
5 x 10^4	0.8958	0.9332	1.1930	1.166	1.209
2 x 10^5	0.8746	0.9422	1.1900	1.178	1.139
5 x 10^5	0.8751	0.9394	1.2184	____	0.295
1 x 10^6	0.8787	0.9434	1.2082	____	0.350

The two-dimensional numerical simulation could not to capture the *drag crisis* as expected, because the three-dimension effects of the boundary layer transition cannot be obtained.

Before the drag crisis, the results of LES presented good accuracy with the experimental results, as shown in Fig. 4. The results of $\overline{C}_D$ obtained with DES and URANS are very close. However these methodologies underestimate the drag force over the cylinder.

The last two simulate cases are on the drag crisis region and it can be observed that the three methodologies cannot preview the decrease of the drag coefficient with the increase of the Reynolds number. Therefore the numerical results do not reproduce the experimental results at the drag crisis region. It is well known that the drag crisis is associated with the boundary layer transition to the turbulent regime and that at this kind of phenomena the three-dimensional effects prevail. It was not expected that a two-dimensional code could reproduce this behavior without any specific correction. The main difference of the LES and DES results when compared with URANS can be due to the turbulence model used to calculate the turbulent viscosity.

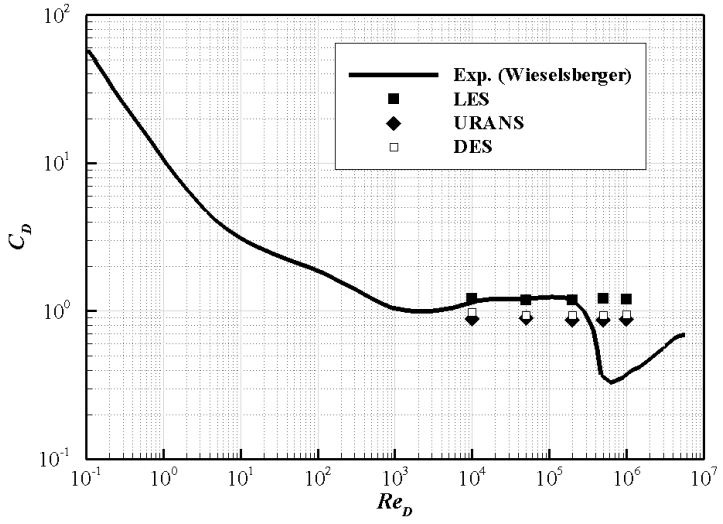

Figure 4. Drag coefficient as function of the Reynolds number.

The drag force over the cylinder is produced by the viscous forces (C_{Df}) and by the asymmetric pressure distribution along the surface of the cylinder (C_{Dp}):

$$C_D = C_{Dp} + C_{Df} \tag{13}$$

However the effects of viscous friction forces become negligible beyond $Re_D \geq 10^3$, (Zdravkovich, 1997). The Smagorinsky model used with the LES methodology has the characteristic of to overestimate the turbulent viscosity (ν_t) in the regions near the cylinder wall. In the vortices street region the ν_t is substantially smaller than the calculated with DES and URANS. Due to the LES modeling be less viscous, at this region the downstream pressure is lower than that of the other models. That imply a higher adverse pressure gradient that increases the total drag force.

Table 2. Drag coefficient obtained with the three methodologies and compared with the experimental ones.

Re_D	Strouhal Number (St)			
	Present Work			Roshko (Zdravkovich, 1997)
	URANS	DES	LES	Curve Fit (Exp. Data)
1 x 10^4	0.1877	0.2125	0.2507	0.2117
5 x 10^4	0.1752	0.2125	0.2569	0.2119
2 x 10^5	0.1877	0.2125	0.2451	0.2120
5 x 10^5	0.1877	0.2125	0.2463	0.2120
1 x 10^6	0.1857	0.2125	0.2403	0.2120

The Strouhal number (St), the dimensionless vortices shedding frequency, is shown in Tab. 2. Experimental data obtained by Roshko (1967) are also presented. The results of St obtained with DES presents very good agreement with the experimental results. This parameter is constant, for this Reynolds number range which is maintained around 0.2. The difference among the numerical results can be associated with the characteristics of each turbulence model, as reported by other authors.

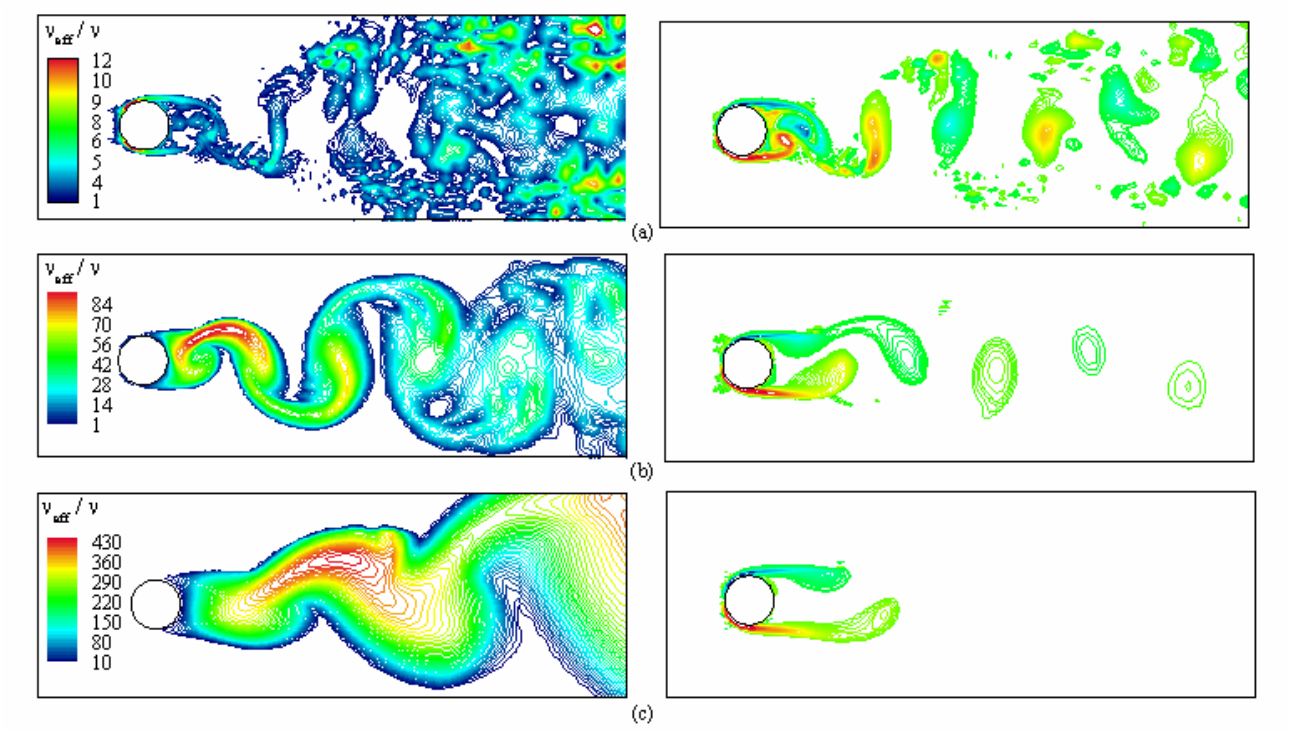

Figure 5. Instantaneous viscosity and vorticity fields obtained for $Re_D = 1.0 \times 10^4$ for: LES (a), DES (b) and URANS (c).

The methodology URANS is not adequate to analyze transient behavior of the flow, due to the high level of turbulence viscosity associated to this class of models. Only the average behavior of the flow can be obtained and consequently, it captures less physical phenomenon. In fact the Strouhal number obtained with URANS methodology is under predicted when compared with experimental results, as presented in Tab. 2. Large Eddy Simulation methodology,

in the other hand, presents a small level of turbulence viscosity as can be observed in Fig. 5-a. As a consequence the Strouhal number is over predicted, presenting Strouhal number greater than the experimental results. The DES methodology, with is a kind of URANS and LES blending presents an intermediated level of turbulent viscosity (see Fig. 5-b. The Strouhal number is very well calculated with this hybrid methodology, as can be observed in Tab. 2.

Figure 5 shows effective viscosity and vorticity fields for flow at $Re_D = 1.0 \times 10^4$. The effective viscosity near wall computed by URANS model has the same magnitude as the molecular viscosity, for regions behind the cylinder, the wake region, the effective viscosity assumes high values. This inhibits the vortex shedding as can be observed in vorticity field in Fig. 5-c. Differently the effective viscosity computed by Smagorinsky model has high values near parietal regions. This is due to the fact that the Smagorinsky model does not dump the turbulent viscosity close to walls. However, for regions away from walls LES capture a large spectrum of physical phenomena. We can observe in Fig. 5-a that structures behind the cylinder, in vorticity fields calculated by LES methodology, are more coherent.

DES methodology shows an intermediary behavior, between LES and URANS. The effective viscosity computed by S-A based DES model, in the wake region, is less intense than values calculated by the standard S-A model, a consequence we can visualize vortices being transported by the fluid flow behind the cylinder; however the DES is still more viscous than the LES model in this flow region. The S-A based DES model computed maximum effective viscosity values in the zone nearest solid walls (like Smagorinsky model). But these high viscosity values are concentrated only over a small wall region where high stress rates appear. For all other interface points DES provides results similar to URANS model, i.e., the turbulent viscosity is near zero.

6. Conclusions

In the present work, it was shown that the extension of *Immersed Boundary Method/Virtual Physical Model* (IB/VPM) to simulation unsteady, viscous incompressible flows at high Reynolds numbers. A brief comparative study between different turbulence models (S-A based URANS, S-A based DES and Smagorinsky-LES) implemented with the IB method is also presented. The obtained results is considered quite good for a *2D* code. The main parameters of fluid flow across a cylinder: Strouhal number, drag and lift coefficients is predicted with good accuracy for the region up to *drag crisis*. Simulations at supercritical Reynolds numbers present poor results, however, we believe that a *2D* simulation without a wall-layer model is incapable to give realistic results for this Reynolds number region. For this reason the methodology seems to be suitable for investigate problems at high Reynolds evolving complex geometry, e.g., flows over airfoil in transient pitching motions.

7. Acknowledgements

The authors acknowledge CNPq for the financial support provided for this work and the School of Mechanical Engineering of the Federal University of Uberlândia for the technical support.

8. References

Arruda, J. M. (2004). Modelagem Matemática de Escoamentos Internos Forçados Utilizando o Método da Fronteira Imersa e o Modelo Físico Virtual. Ph. D. thesis, Universidade Federal de Uberlândia.

Chorin, A. (1968). Numerical solution of the Navier-Stokes equations. Math. Comp. 22, 745–762.

Germano, M. (1986). A proposal for a redefinition of the turbulent stresses in filtred navier-stokes equations. Phys. Fluids 29(7), 2323–2324.

Kapadia, S. and Roy, S. (2003). Detached eddy simulation over a reference ahmed car model. In Proceedings of the 41st Aerospace Sciences Meeting and Exhibit, Number AIAA-2003-0857.

Kim, J., Kim, D. and Choi, H. (2001). An immersed-boundary finite-volume method for simulations of flow in complex geometries. Journal of Computational Physics 171, 132–150.

Lima e Silva, A. L. F., Silva, A. R. and Silveira-Neto, A. (2004). Numerical simulations of two-dimensional complex flows over bluff bodies using the imersed boundary method. Unpublished.

Lima e Silva, A. L. F., Silveira-Neto, A. and Damasceno, J. J. R. (2003). Numerical simulation of two dimensional flows over a circular cylinder using the immersed boundary method. Journal of Computational Physics 189, 351–370.

Oliveira, J. E. S., Lima e Silva, A. F. L. Guimarães, G. and Silveira-Neto, A. (2004). Simulação numérica do escoamento a baixo reynolds sobre um cilindro de diâmetro variável usando MFI / MFV. 10th Brazilian Congress of Thermal Sciences and Engineering.

Peskin, C. S. (1977). Numerical analysis of blood flow in the heart. Journal of Computational Physics 25, 220–252.

Roshko, A. (1967). Experiments on the flow past a circular cylinder at very high Reynolds number, Journal of Fluid Mechanics, Vol. 10, pp. 345–-356.

Schlichting, H. (1979). Boundary-Layer Theory. New York, USA: McGraw-Hill Book Company.

Schneider, G. E. and Zedan, M. (1981). A modified strongly implicit procedure for the numerical solution of field problems. Numerical Heat Transfer 4, 1–19.

Shur, M., Spalart, P., Strelets, M. and Travin, A. (1999). Detached-eddy simulation of an airfoil at high angle of attack. In 4th International Symposium on Engineering Turbulence Modelling and Measurements, pp. 669–678. Elsevier, Amsterdam.

Silva, A. R., Carvalho, G. B. Lima e Silva, A. F. L., Mansur, S. S. and Silveira-Neto, A. (2004). Modelagem matemática e simulação numérica de escoamentos sobre corpos móveis utilizando-se o método da fronteira imersa. In Submitted to Proceedings of the 10o Brazilian Congress of Thermal Sciences and Engineering.

Silveira-Neto, A. (2003). Introdução Turbulência dos Fluidos, Apostila do Curso de Pós-Graduação em Eng. Mecânica. LTCM/FEMEC/UFU.

Silveira-Neto, A., Mansur, S. S. and Silvestrini, J. M. (2002). Equações da turbulência: Média versus filtragem. In Anais da 3o Escola de Turbulência, Florianópolis - SC.

Smagorinsky, J. (1963). General circulation experiments with primitive equations. Monthly Weather Review 91, 99– 164.

Spalart, P. R. and Allmaras, S. R. (1994). A one-equation turbulence model for aerodynamic flows. La Recherche Aérospatiale 1, 5–21.

Spalart, P. R., Jou, W.-H., Strelets, M. and Allmaras, S. R. (1997, Aug 4-8). Comments on the feasibility of LES for wings, and on a hybrid RANS/LES approach. In Advances in DNS/LES, 1st AFOSR Int. Conf. On DNS/LES, Columbus, Ohio. Greyden Press.

White, F. M. (1991). Viscous Fluid Flow. New York, USA: McGraw-Hill Book Company.

Zdravkovich, M. M. (1997) Flow around circular cylinders, vol. 1: Fundamentals, New York, Oxford University Press.

9. Responsibility notice

The authors are the only responsible for the printed material included in this paper.